79-4034

Observations of the Oscillatory Behavior of a Confined Ring Vortex

M. P. Escudier* and P. Merkli†
Brown Boveri Research Center, Baden, Switzerland

Ring chambers with annular inflow and outflow through a radial exit tube find wide application in axial-flow turbomachinery as exit chambers to collect and divert the throughflow off-axis. Visual observations and detailed measurements of the flow in an idealized model exit chamber reveal that the flow in the ring is dominated by the vortex generated by the annular inflow. Coriolis forces, arising as a result of the longitudinal curvature imposed on the basic swirling flow, cause the vortex to adopt a helical form within the confines of the ring. Also, an interaction between the two ends of the vortex within the exit tube gives rise to oscillations of the flow which are strongly periodic for certain values of the ratio of the annular width t to the ring radius R. The periodic oscillations are characterized by a constant Strouhal number $fR/V \approx 0.03$, where f is the fundamental frequency and V the inflow velocity. Although the flow oscillations can be suppressed by installing a splitter plate in the exit tube, when the vortex ends are separated and so cannot interact, the splitter plate has no direct influence on the vortex, the spatial structure of which is largely unaltered.

Nomenclature‡

D = diameter of ring model, m
f = frequency of oscillation, Hz
H = hydraulic diameter of inlet annulus = $2t$, m
$\dot{m}$ = mass flow rate, kg/s
p = mean static pressure, mm Hg
p' = rms value of fluctuating pressure, mm Hg
p_0 = stagnation pressure, mm Hg
q = dynamic pressure, mm Hg
r = radial coordinate, m
R = radius of ring cross section, m
Re = Reynolds number $\equiv \rho VH/\mu$, –
St = Strouhal number $\equiv fR/V$, –
t = width of annular inlet, m
u = radial velocity component, m/s
v = swirl velocity component, m/s
V = average velocity in annulus (reference velocity), m/s
w = axial velocity component, m/s
W = average axial velocity component, m/s
Γ = circulation, m^2/s
θ = angular position, deg
μ = dynamic viscosity, kg/m/s
ν = kinematic viscosity, m^2/s
ρ = density, kg/m^3

Introduction

A PROBLEM inherent in the design of many types of axial-flow turbomachinery is that of collecting the throughflow and diverting it away from the machine's main axis. A commonly encountered solution to this problem is the use of a ring chamber with annular inflow, such as that shown schematically in Fig. 1. In practice, the ring cross section may be noncircular, for reasons unrelated to considerations of fluid mechanics, and the axial inflow complicated by such upstream influences as a diffuser or blading stages. Previous work[1] on the performance of ring-type exit chambers has been largely concerned with geometries close to those used in practice and with the question of pressure losses. In contrast, the present work is concerned with the oscillatory nature of the flow, and has been restricted to the study of an idealized geometry where flow conditions and geometric parameters can be precisely specified.

The problems of noise, structural vibration, and combustion instabilities, which can result from periodic fluctuations in the flow, can be particularly severe in large turbomachines where vast amounts of energy are available to feed the fluctuations. The understanding of the causes of periodic instabilities in turbomachinery and their avoidance or suppression is the motivation for the present investigation.

The flow in a ring chamber is dominated by the vortex generated in the ring by the tangential inflow. We report experiments, with both water and air as working fluids, which reveal the structure of the vortex and the complex flow phenomena associated with it, with emphasis on the periodic nature of the flow. Much effort has gone into trying to understand confined vortex flows in straight tubes in view of their importance to such diverse applications as the cyclone separator, vortex whistle, fluidic vortex valve, Ranque-Hilsch tube, gas-core nuclear rocket, and, recently, the vortex wind turbine. An extensive review of the subject of confined vortex

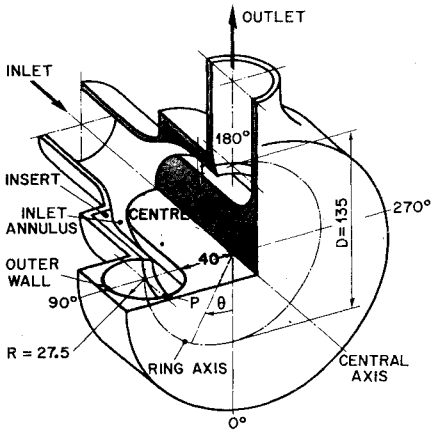

Fig. 1 Schematic diagram of exit-chamber model (dimensions in mm).

Received June 14, 1978; revision received Nov. 3, 1978.

Index categories: Nonsteady Aerodynamics; Aeroacoustics.

*Leader, Fluid Mechanics Research Group.

†Scientist, Fluid Mechanics Research Group.

‡Only the basic quantities used are listed here; other notation is introduced as required.

flows is given by Lewellen,[2] who discusses both the current state of theoretical and experimental knowledge and also technical applications. Although some observations of the oscillatory behavior of vortex flows have been reported by Vonnegut,[3] Chanaud,[4] and Cassidy and Falvey,[5] among others, there seems to be no direct connection with the effects discussed here. In common with the earlier studies, however, is the fact that the periodic phenomena are characterized to a large extent by a constant Strouhal number, that is, by a linear relationship between frequency and a characteristic velocity.

Experimental Arrangement

The layout and principal dimensions of the model investigated are as shown in the cutaway diagram in Fig. 1. It may also be noted that the inlet and outlet pipes have the same diameter (55 mm) as the ring cross section. The model was designed to permit measurements of the wall pressure in the ring at any point around a circle through P (in Fig. 1) in a plane orthogonal to the central axis. Construction is largely of plexiglas to permit flow visualization and LDV measurements in water. The principal geometric variable is the width t of the inlet annulus, which can be changed through the use of sleevelike inserts. The largest number of measurements has been made for $t=8.5$ mm (i.e., $t/R=0.31$), since in this case periodic fluctuations of the flow are defined most clearly. Experiments have also been carried out for inlet annuli with $t=4.5$, 5.05, 6.6, 13.5, and 16 mm, corresponding to values of t/R ranging from 0.16 to 0.58. In addition to varying t/R, it is possible to study the influence on the flow of a dividing disk at the 0 deg position (forward stagnation plane) and of a splitter plate at the 180-deg exit position.

Observations and Measurements in Water

A. Flow Visualization

For $t/R=0.31$ at the maximum achievable flow rate (about 5.5 ℓ/s, corresponding to a Reynolds number of 4.10^4), the existence of a strong vortex in the ring is immediately apparent through the presence of air and water-vapor bubbles marking the vortex core. The principal source of these bubbles appears to be gaseous cavitation in the core, although air bubbles swept into the vortex from elsewhere in the flow system are also centrifuged into the core where they accumulate and coalesce. At low flow rates, the bubbles tend to remain discrete and "dance" to and fro along the core. As the flow rate increases, sufficient bubbles accumulate to form a continuous hollow core with a diameter of about 10% of the vortex' outer diameter (i.e., 0.2 R). The axial and side-view photographs in Fig. 2 show the characteristic "helical" shape of the core, which is observed to be independent of flow rate. Around the whole ring there are about three complete turns of the helix, the axis of which is displaced slightly outward from that of the ring. The helical shape is a result of the Coriolis forces induced in the swirling flow as it is bent in the ring. The turning of the ends of the vortex core into the exit tube is also evident from Fig. 2a.

The vortex is not stable but oscillates periodically about the central axis of the model with an angular amplitude of the core of about 20 deg. The period is well defined and easily estimated with a stopwatch at all flow rates for which the core is visible. In Fig. 3, the variation of frequency f with the mass flow rate $\dot{m}$ is seen to be closely linear, giving a constant Strouhal number $fR/V=0.026$. It is of interest to note that the alternative definition for the Strouhal number $f\rho D^3/\dot{m}$ would have the value 1 in this case.

As the annulus width is varied, the most notable change in flow structure is that the helicity of the vortex decreases as t/R increases, though with little change in pitch. The flow remains strongly unstable whether t is increased or decreased, but is less clearly periodic than for the intermediate annulus with $t/R=0.31$.

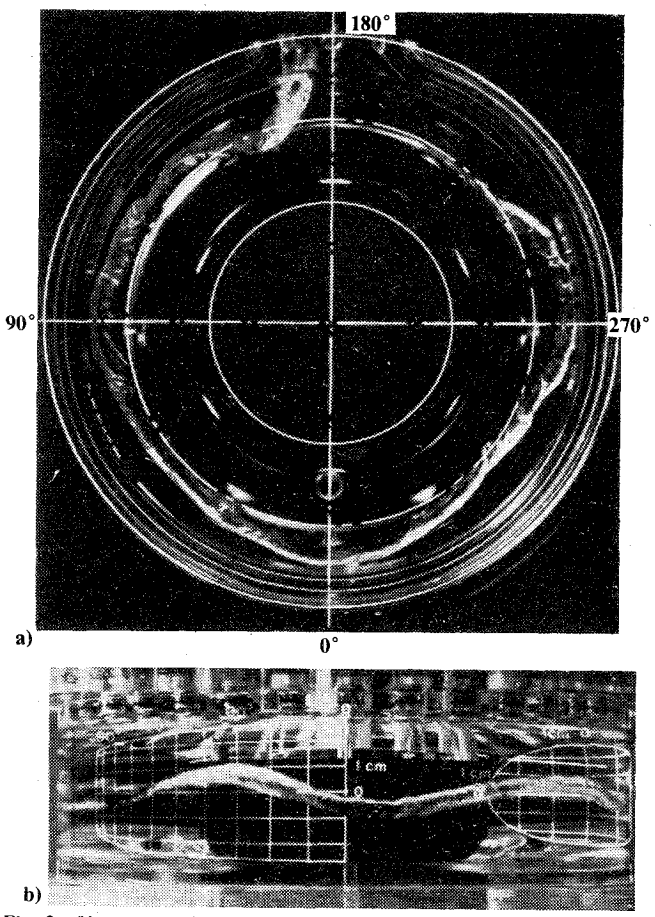

Fig. 2 Vortex core in water flow: a) Axial view; b) Side view from 0 deg.

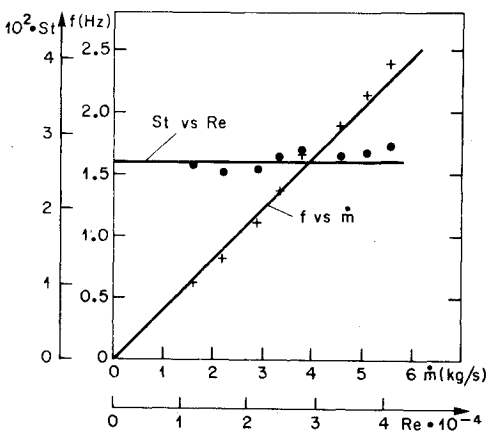

Fig. 3 Vortex oscillation frequency f and Strouhal number St measured in water flow.

Installation of a dividing disk at the 0 deg position has little influence on the appearance of the vortex, and the flow is still periodic with essentially the same constant Strouhal number as observed in its absence. Dye injected directly into the vortex core from holes in the disk face is rapidly diffused throughout the flow. However, it is readily apparent that dye is sucked first from the hole on one side of the disk, and then from that on the other. A further observation is that when the dye supply to the disk is cut off, the core zone takes much longer to clear than the fluid around it.

In contrast to the negligible stabilizing influence of the dividing disk at $\theta=0$ deg, the flow is quite effectively stabilized by a splitter plate installed in the exit tube in the plane of symmetry of the model, although the helical shape of

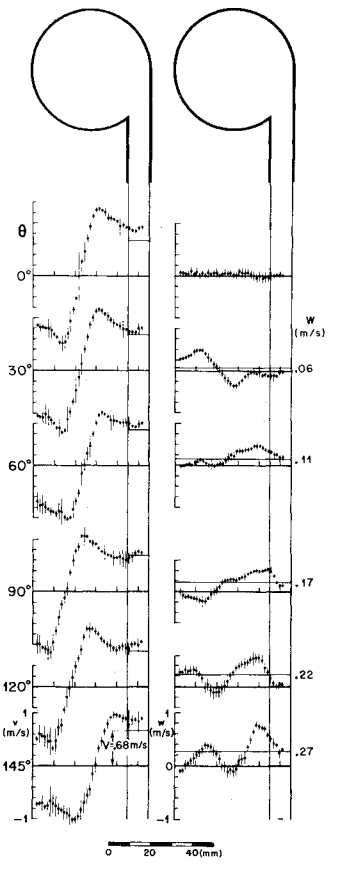

Fig. 4 LDV measurements of swirl- (v) and axial-velocity (w) components in water flow; V = average inflow velocity and W = average axial velocity.

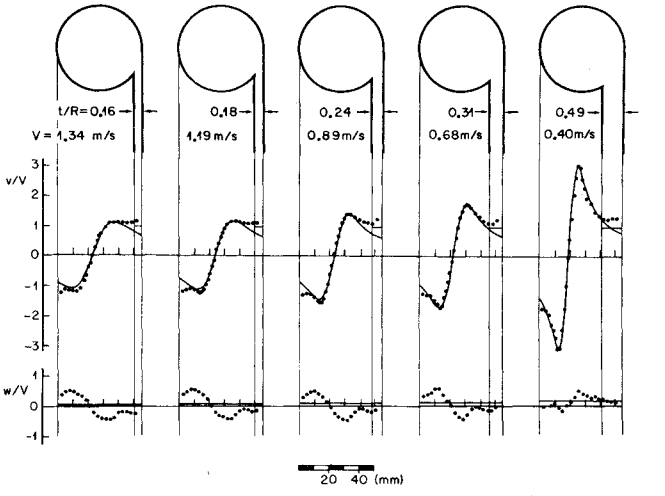

Fig. 5 Swirl- and axial-velocity profiles measured at $\theta = 30$ deg for various inlet widths. Solid curves shown for comparison with swirl profiles represent Burgers' analysis.

the core is again unchanged. The influence of the splitter plate suggests that the periodic nature of the flow arises from an interaction of the two ends of the vortex core where they meet in the exit tube. Strength is added to this hypothesis by the results of preliminary experiments carried out in a straight vortex tube of similar dimensions to the model under discussion. In the linear model, the ends of the vortex core do not meet, and the vortex is quite stable. To further clarify the role of the exit, experiments are under way involving the interaction of two vortices of opposite sign confined within a straight tube.

B. Laser Doppler Velocimeter (LDV) Measurements

The sensitivity of a vortex to probe disturbance dictates the use of an optical technique, such as LDV, for measurements within the flow. The difficulty of making such measurements, as a result of the necessity to correct for optical aberrations introduced by the curved walls of the model, cannot be overemphasized. Nevertheless, with the aid of specially designed correction lenses,[6] measurements have been made of the swirl and axial (taken here to mean in the θ direction) components of the velocity for the plane containing the ring axis where the optical problems are the least severe. The measurements were made in deionized water seeded with 5.7 μ Dow latex spheres using the BBC-Goerz LDV system. A 40-MHz Bragg cell was incorporated into the system to permit determination of both the magnitude and direction of each velocity component.

For $t/R = 0.31$, a set of velocity profiles, measured at 30 deg intervals for a flow stabilized with an exit-tube splitter plate, is given in Fig. 4. The flow rate is about 30% of maximum, since above this value bubbles produced by cavitation begin to interfere with the measurements. As changes of other quantities such as the loss coefficient with Reynolds number are not great, the qualitative appearance of these profiles may be assumed to be representative of higher flow rates also. At each radial position, 100 discrete measurements are made of each component. The plotted points represent the means of these values, and the vertical lines the corresponding standard deviations. Large local deviations may be attributed to passage of an air bubble through the flow system, reflections from dust particles on the surfaces of the lenses and the model, or shifts in the profile due to instabilities which are not fully suppressed by the splitter plate.

In assessing these measurements, it must be borne in mind that they were obtained in a single plane, but represent a strongly three-dimensional flowfield and are, therefore, largely of qualitative value. This point is emphasized by the axial flow velocity profiles which are far from symmetrical. Nevertheless, the swirl-velocity profiles show more or less the expected form, with an approximately linear (solid-body) core surrounded by a region of decreasing velocity, although of shallower gradient than would be the case for a potential vortex. The subsequent increase of the swirl velocity near the inner wall, even exceeding the mean inlet velocity, may be attributed to blockage of the inlet flow by the vortex.

The axial-flow component of velocity is even more complicated than the swirl, with regions of backflow compensated for by velocities far in excess of the average velocity at any angular position. The presence of backflow, typical of many vortex flows as a result of the low core pressure, is presumably responsible for the persistence of dye and air bubbles in the core zone mentioned earlier.

Extensive LDV measurements have been performed for inlet annuli other than $t/R = 0.31$. The zero-crossing position of the swirl component clearly shows the increasing helicity with decreasing t/R which is observed visually. Otherwise, the qualitative changes in the swirl velocity are as expected, as discussed later where a comparison with Burgers'[7] theoretical solution is discussed. As far as the axial profiles are concerned, the only common feature is the strong departure from uniformity, although no pattern for the nonuniformity is apparent.

C. Comparison of LDV Measurements with Burgers' Solution

Since there is no possibility of a complete theoretical analysis of the flow in a ring chamber, it is interesting to compare the measured tangential velocity distributions with an exact solution of the Navier-Stokes equations for a somewhat simplified situation. The simplest possible solution[7] is that for an axisymmetric vortex with a uniform axial velocity w which increases linearly with axial position x:

$$v = (\Gamma/2\pi r)[1 - \exp(-ar^2/2\nu)] \quad \text{and} \quad w = 2ax$$

where a and Γ are constants, $2a$ being the axial velocity

gradient, Γ the circulation at infinity, and ν the kinematic viscosity. To make the comparison, values of Γ and the ratio a/ν were chosen to insure exact agreement between the measurements and Burgers' result at the velocity maximum.§ The vortex center ($r=0$) is taken as the point where the measured velocity is zero i.e., to compensate for the helicity it is necessary to shift the theoretical vortex center away from the ring axis. The result of the comparison for velocity distributions measured at $\theta=30$ deg for values of t/R between 0.16 and 0.49 is given in Fig. 5. The measured profiles have been normalized with respect to the mean inflow velocity V, calculated from the mass flow rate and annulus area. It is apparent that the flattening of the profiles at the outer edge of the vortex cannot be represented by Burgers' profile, which has the hyperbolic potential flow solution as its asymptote. As already mentioned, Burgers' result was obtained assuming a uniform, linearly increasing axial velocity in a straight tube, whereas the measured axial velocity profiles included in Fig. 5 are clearly far from uniform. More recently, Donaldson and Sullivan[8] have reported families of solutions for axisymmetric vortex flows which include the possibility of backflow for swirl profiles having much the same appearance as Burgers'. However, such solutions cannot easily be compared with measurements and, in any case, do not include the effects of the surface boundary layers which strongly influence the problem. Consequently, we accept Burgers' solution merely as a reasonable representation of the tangential velocity distribution, recognizing that it is totally deficient with respect to the axial flow.

Observations and Measurements in Air

A. Pressure Fluctuations

For $t/R=0.31$, frequency spectra for the fluctuating component of the wall pressure were measured at various flow rates as a function of the angular position θ (for definition of the measuring point P and the angle θ, see Fig. 1 and the section "Experimental Arrangement"). The data shown in Fig. 6 for $\theta=30$ deg are typical. The results are consistent with the observations in water discussed earlier and, in particular, with the plot of f against $\dot{m}$ (Fig. 3)—each spectrum is dominated by a peak at a frequency f which varies more or less linearly with flow rate yielding a Strouhal number $St\cong 0.029$. At some angular positions, several harmonics of this fundamental frequency can also be detected, as is discussed in more detail below.

The angular variation of the fluctuating pressure, measured in narrow frequency bands centered on the fundamental frequency and its first two harmonics, is shown in Fig. 7 for the maximum achievable flow rate. The data give the impression of a standing wave, with pressure maxima at about 30, 75, and 120 deg and nodes at 0, 55, 95, and 180 deg (for the fundamental). Similar measurements at lower flow rates show essentially the same angular distribution, but with correspondingly lower frequencies and amplitudes.

The stabilizing effect on the vortex oscillation of a splitter plate installed in the exit pipe was already apparent in the water flow observations for $t/R=0.31$, and is clearly confirmed by the frequency spectra shown in Fig. 8 which contain no significant peaks. Also consistent with the earlier observations are the measurements for the model with a dividing disk at $\theta=0$ deg, which give frequency spectra in the range 0-500 Hz little different from the case without the disk. The angular distribution of the fluctuating pressure, after bandpass filtering as just described, again suggests a standing wave pattern, but with the first pressure maximum shifted to the disk face.

§We do not use the kinematic viscosity of the fluid itself directly. Rather, ν should be interpreted here in the sense of an eddy viscosity though, in fact, we do not separate the parameters a and ν.

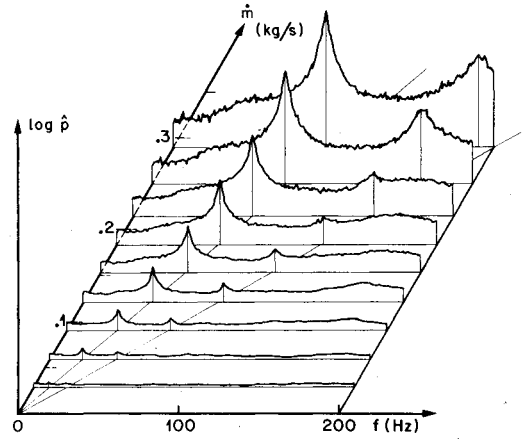

Fig. 6 Frequency spectra of fluctuating pressure at $\theta=30$ deg.

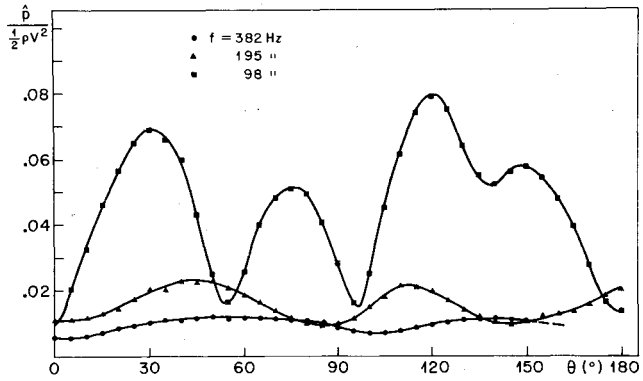

Fig. 7 Angular distribution of fluctuating pressure after bandpass filtering.

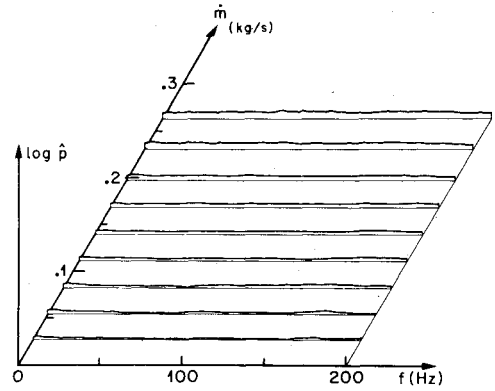

Fig. 8 Frequency spectra of fluctuating pressure at $\theta=30$ deg with splitter plate in exit tube.

The strong dependence of the flow characteristics on the relative width of the inlet annulus may be assessed from the frequency spectra plotted in Fig. 9 for values of t/R between 0.16 and 0.49. In all cases, periodic flow-dependent fluctuations are in evidence, but less well defined than for $t/R=0.31$. Also, in a further experiment with $t/R=0.58$, no such oscillations could be detected. However, we do find that for a wide range of inlet annuli, the frequencies of the periodic fluctuations in pressure belong to a single family. This is shown in Fig. 10a where the Strouhal number $St\equiv fR/V$ is plotted against the Reynolds number $Re\equiv\rho VH/\mu$ for $t/R=0.24$, 0.31, 0.40, and 0.49. The fundamental oscillation frequency, determined from numerous spectra (at various θ values) similar to those shown in Fig. 9, gives the result $St\cong 0.03$, independent of t/R and only weakly

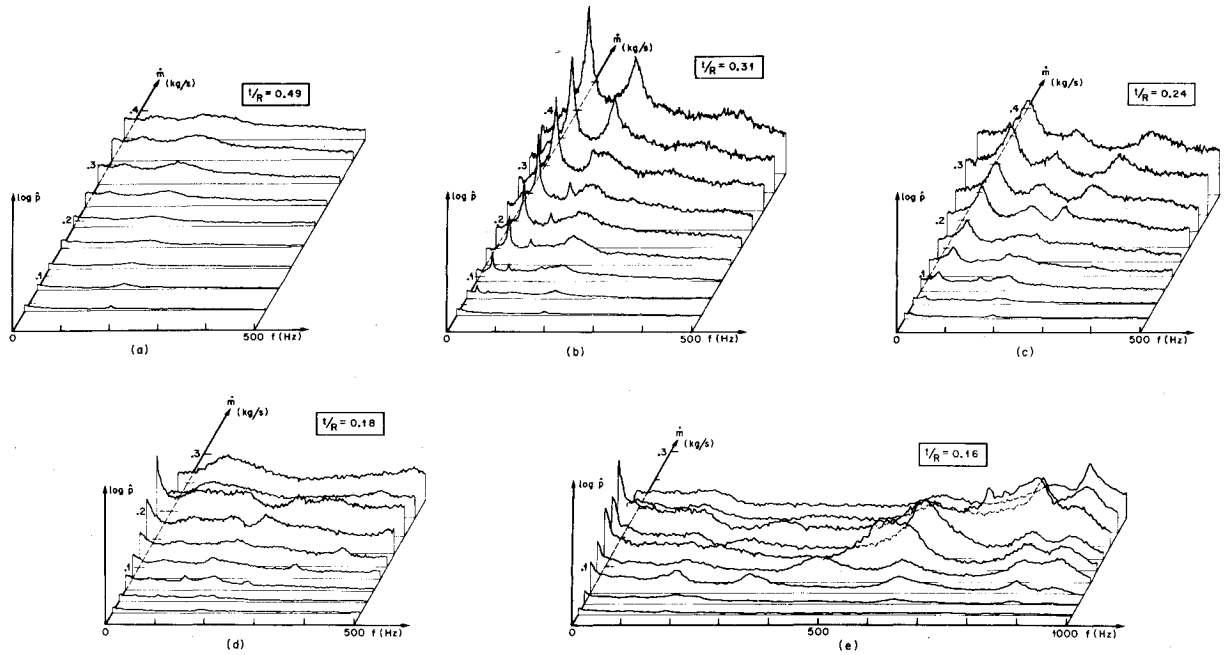

Fig. 9 Frequency spectra of fluctuating pressure at $\theta = 30$ deg for various inlet-annulus widths.

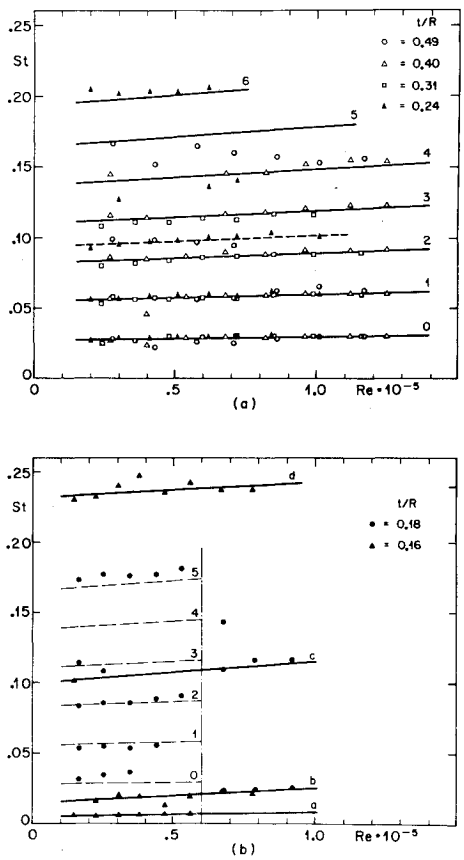

Fig. 10 Dependence of Strouhal number on Reynolds number: a) $t/R \geq 0.24$, b) $t/R < 0.24$.

dependent on Re. The first harmonic of f is also well defined, and harmonics up to sixth order are detectable, although much less well defined than the fundamental and first harmonic. Clearly, some points fall on curves, such as the dashed line between the second and third harmonics, which are not harmonically related to the fundamental.

Deviations of another kind are found for $t/R < 0.24$, as shown in Fig. 10b. For $Re < 5 \cdot 10^4$, the data for $t/R = 0.18$ follow essentially the same pattern as those for the wider annuli. Above this "critical" Reynolds number, however, and for $t/R = 0.16$ in general, periodic fluctuations still occur, but with Strouhal numbers following no clear pattern.

In addition to peaks in the spectra which occur at flow-dependent frequencies, there are fixed-frequency peaks which correspond to resonances at the acoustic eigenfrequencies of the ring model excited by the flow. These eigenfrequencies have been discussed in some detail by Merkli[9] who shows that they may be calculated by treating the ring chamber and exit pipe as a T-tube. Frequencies calculated using Merkli's analysis are indicated below the abscissa in Fig. 11, which covers an extended frequency range compared to Fig. 9e, and are seen to be in good agreement with the measurements.

The interaction between flow-excited acoustic resonances and, for example, vortex shedding has received considerable attention in the literature. Although such an interaction is often associated with the phenomena of frequency locking and hysteresis,[10,11] this is not observed in our ring-chamber experiments. There is, however, something of an amplitude enhancement when the frequency corresponding to the vortex oscillation is close to an acoustic eigenfrequency. This can be seen to a certain extent from the frequency spectra in Fig. 9e and more clearly in Fig. 12, which shows the variation with Reynolds number of the fluctuating pressure level (rms value normalized with respect to the dynamic head q in the inlet annulus) for $t/R = 0.31$ and 0.16. In the first case, the vortex frequencies all fall below the acoustic eigenfrequencies¶ within the range of Reynolds numbers achievable in our apparatus and there is no interaction. For $t/R = 0.16$, on the other hand, the vortex frequency for $Re = 4.5 \cdot 10^4$ is about 600 Hz, which corresponds to the fundamental acoustic eigenfrequency for a combined resonance of the torus and exit tube.[9] The interaction in this case is seen to result in an increase in the fluctuating pressure of about 100%. A further feature of interest is that the oscillation has a bistable character. As may be seen from Fig. 13, the fluctuating pressure switches randomly between two well-defined levels, a lower (normal) level and a higher (enhanced) one. This rather weak interaction is probably due to the fact that although the frequencies are the same, there is a mismatch in the angular

¶There is no interaction with the Helmholtz resonance, which has no spatial variation.

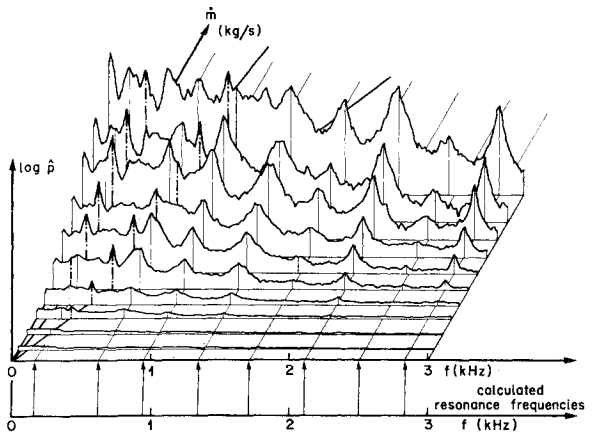

Fig. 11 Frequency spectra of fluctuating pressure at $\theta = 5$ deg for model with disk, together with calculated acoustic eigenfrequencies ($t/R = 0.16$).

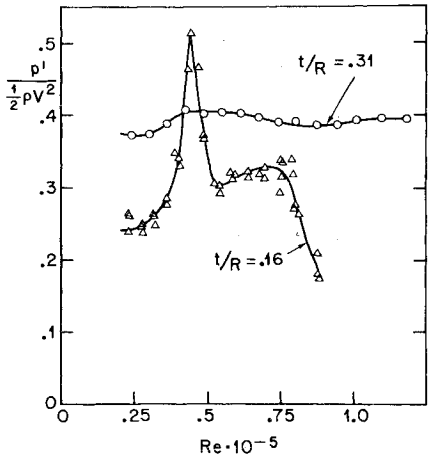

Fig. 12 Variation with Reynolds number of normalized rms fluctuating pressure at $\theta = 30$ deg.

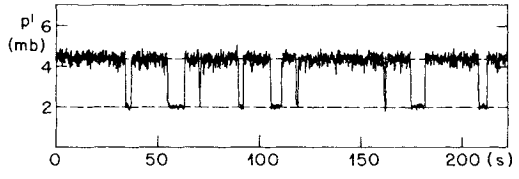

Fig. 13 Bistable behavior of fluctuating pressure for $t/R = 0.16$.

distributions of the fluctuating pressure for the flow oscillation and the acoustic resonance, i.e., there is a phase mismatch.

B. Mean Static-Pressure Distribution

The angular distribution of the time-averaged static pressure p is plotted in Fig. 14 for $t/R = 0.31$ for the model without flow dividers. The reference pressure p_2 is measured in the inlet tube. The curves for all flow rates are evidently similar, and again reflect the independence with regard to flow rate of the helical shape of the vortex core. Additional data (not shown) obtained with the dividing disk and/or splitter plate installed in the model show variations only slightly different from those of Fig. 14, also again confirming the water flow observation that the basic vortex structure is little affected by such baffles.

C. Total Pressure Distribution at the Model Exit

The distribution of total pressure measured in the model exit plane with the exit tube removed is shown in Fig. 15a. The

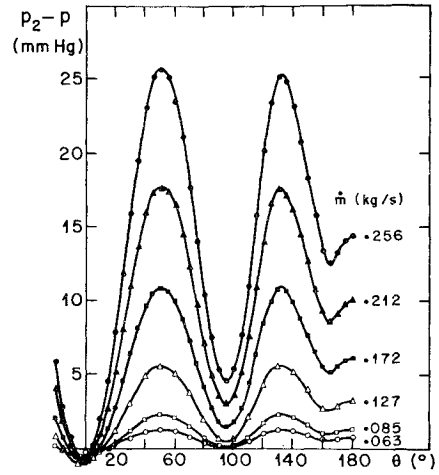

Fig. 14 Angular distribution of mean static pressure for various flow rates.

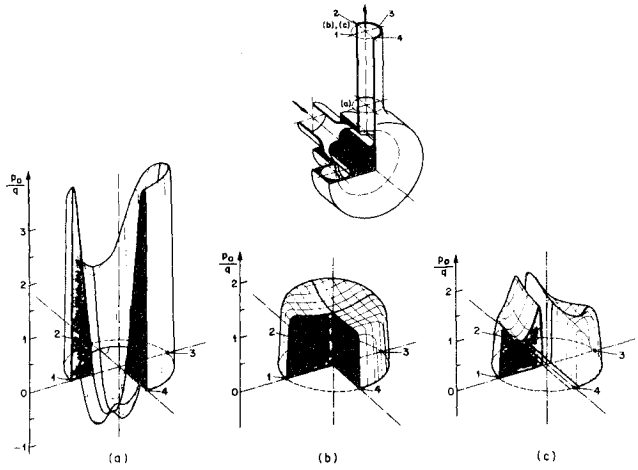

Fig. 15 Distribution of total pressure at: a) entrance to exit tube; b) outlet from exit tube; c) outlet from exit tube for model with splitter plate. Insert of model shows measuring planes.

presence of the two ends of the vortex is clearly indicated by the two minima in the pressure distribution, which are at a level well below the static (i.e., ambient) pressure at the exit plane. This is consistent with visual observations in water which show that the ends of the vortex core do not join together in the torus but turn into the exit tube, as was mentioned previously. Here again the occurrence of backflow is suggested, although measurements with a simple total-head tube in a strongly three-dimensional flow, possibly with reversed flow, must be regarded as qualitative only. The distribution of total pressure at the outlet end of the exit tube, shown in Fig. 15b, is quite flat on the other hand—the degree of mixing that occurs in the exit tube to transform the pressure distribution of Fig. 15a into that of 15b, is remarkable considering that the tube has a length of less that 4 diam. The final pressure distribution, shown in Fig. 15c, was measured at the outlet end of the exit tube with the splitter plate installed. Even in this case where the two ends of the vortex remain separated in the exit tube and the mixing is correspondingly less intense, the vortex is largely diminished in strength at the exit from the tube, although still clearly detectable.

D. Surface-Flow Visualization

Blobs of colored liquid, such as water or light oil, applied to a surface exposed to flow yield streaks which give an impression of the flow close to the surface. Several such streak pictures are shown in Fig. 16 for $t/R = 0.31$ and with a splitter

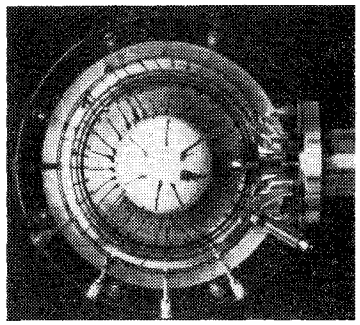
a)

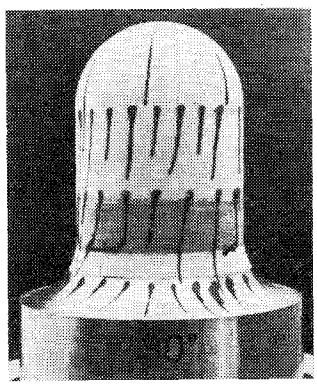
b)

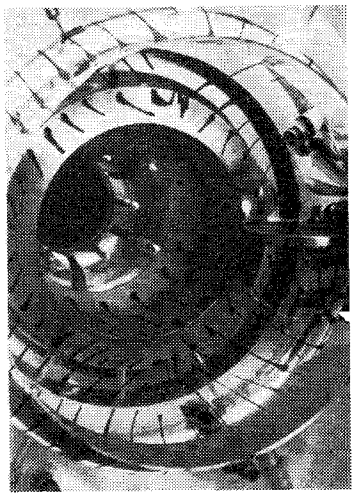
c)

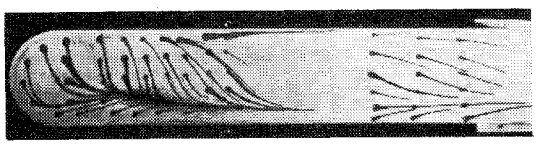
d)

Fig. 16 Surface streaks in disassembled model. a) Axial view from inlet side; b) View of centerbody, outlet to left; c) View into ring towards inlet tube. Outlet and splitter plate to right; d) splitter plate, from left to right.

plate in the exit tube. These pictures support the observations reported in previous sections and, in particular, we note the following:

1) Over much of the torus itself, the orientation of the streaks indicates a strong vortex with a swirl velocity considerably in excess of the axial velocity.

2) Departures from the radial flow direction are seen in Fig. 16a close to $\theta = 0$, 100, and 260 deg, corresponding to the visual observations and LDV measurements in water flow which show the vortex core to come close to the outer wall of

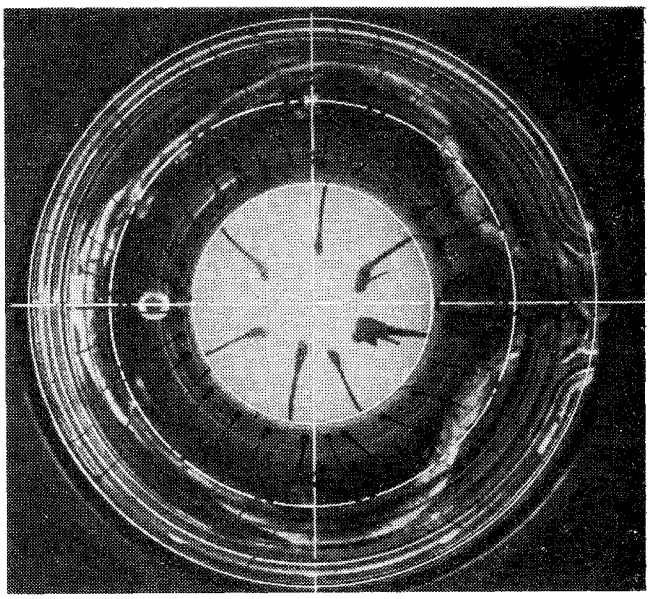
a)

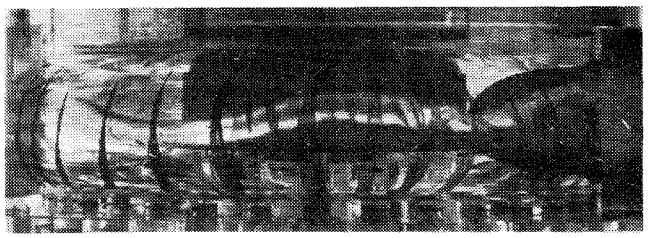
b)

Fig. 17 Superposition of surface streaks for airflow with vortex core in water flow (splitter plate in exit tube): a) axial view toward centerbody and ring; b) side view, exit to right.

the torus and to have sharp bends or kinks at these angles. Superposition of photographs of the vortex core observed in water with the surface streaks in air, as in Fig. 17, reveals that everywhere the streaks are practically orthogonal to the core.

3) From Figs. 16b and 16c it is seen that the flow in the annular inlet is essentially axial except, again, in the vicinity of the vortex kinks where the flow apparently separates from the centerbody which forms the inner wall of the annulus. Other observations, not presented here, show that as the annulus width is increased, the flow in the region 90 deg $< \theta <$ 270 deg is directed somewhat more toward the exit.

4) Figure 16c indicates that, due to the kinks in the vortex, the angle between the streamlines on the two sides of the lip where the inflow meets the vortex, may vary from 0 deg to almost 90 deg.

5) The decrease in vortex strength and rapid evolution of the flow within the exit tube is clearly visible from the change in direction of the streaks on the splitter plate shown in Fig. 16d.

Conclusions

The experimental investigation described here clearly shows the crucial role played by the confined vortex in determining the flow characteristics of a ring-type exit chamber. Although the installation of a splitter plate in the exit tube is effective in suppressing periodic flow fluctuations induced by the vortex, this leaves the basic vortex structure unchanged. Further research is necessary to find ways of influencing the vortex directly and further improving exit chamber design.

Acknowledgments

We gratefully acknowledge the fact that the LDV measurements were made by J. Bornstein and A. Biland, with

advice and help in the early stages from P. Iten and H. Weber. We are also pleased to acknowledge the participation of T. Maxworthy of the University of Southern California in some of the work discussed here.

References

[1]Deych, M. Y. and Zarayankin, A. Y., "Gas Dynamics of Diffusers and Exhaust Ducts of Turbomachines," FTD-MT-24-1450-71, 1972, (translated from Russian).

[2]Lewellen, W. S., "A Review of Confined Vortex Flows," NASA CR-1772, July 1971.

[3]Vonnegut, B., "A Vortex Whistle," *Journal of the Acoustical Society of America*, Vol. 26, Jan. 1954, pp. 18-20.

[4]Chanaud, R., "Observations of Oscillatory Motion in Certain Swirling Flows," *Journal of Fluid Mechanics*, Vol. 21, Jan. 1965, pp. 111-127.

[5]Cassidy, J. J. and Falvey, H. T., "Observations of Unsteady Flow Arising After Vortex Breakdown," *Journal of Fluid Mechanics*, Vol. 41, May 1970, pp. 727-736.

[6]Iten, P. D., private communication, 1976.

[7]Burgers, J. M., "A Mathematical Model Illustrating the Theory of Turbulence," *Advances in Applied Mechanics*, Vol. 1, Academic Press, New York, 1948, pp. 197-199.

[8]Donaldson, C. DuP. and Sullivan, R. D., "Behavior of Solutions of the Navier-Stokes Equations for a Complete Class of Three-Dimensional Viscous Vortices," *Proceedings of the 1960 Heat Transfer and Fluid Mechanics Institute*, Stanford University Press, June 1960, pp. 16-30.

[9]Merkli, P., "Acoustic Resonances in a T-tube," *ZAMP*, Vol. 29, May 1978.

[10]Chen, Y. N., "Flow-Induced Vibration and Noise in Tube-Bank Heat Exchangers Due to von Karman Streets," *Transactions of ASME, Journal of Engineering for Industry*, Feb. 1965, pp. 134-146.

[11]Parker, R. and Pryce, D. C., "Wake Excited Resonances in an Annular Cascade: An Experimental Investigation," *Journal of Sound and Vibration*, Vol. 37, 1974, pp. 247-261.